the Geode
the Geode

MINSA
Mineralogical Association of South Africa
A division of the GSSA

New takes on old analytical tools: this is not your parents' XRF...

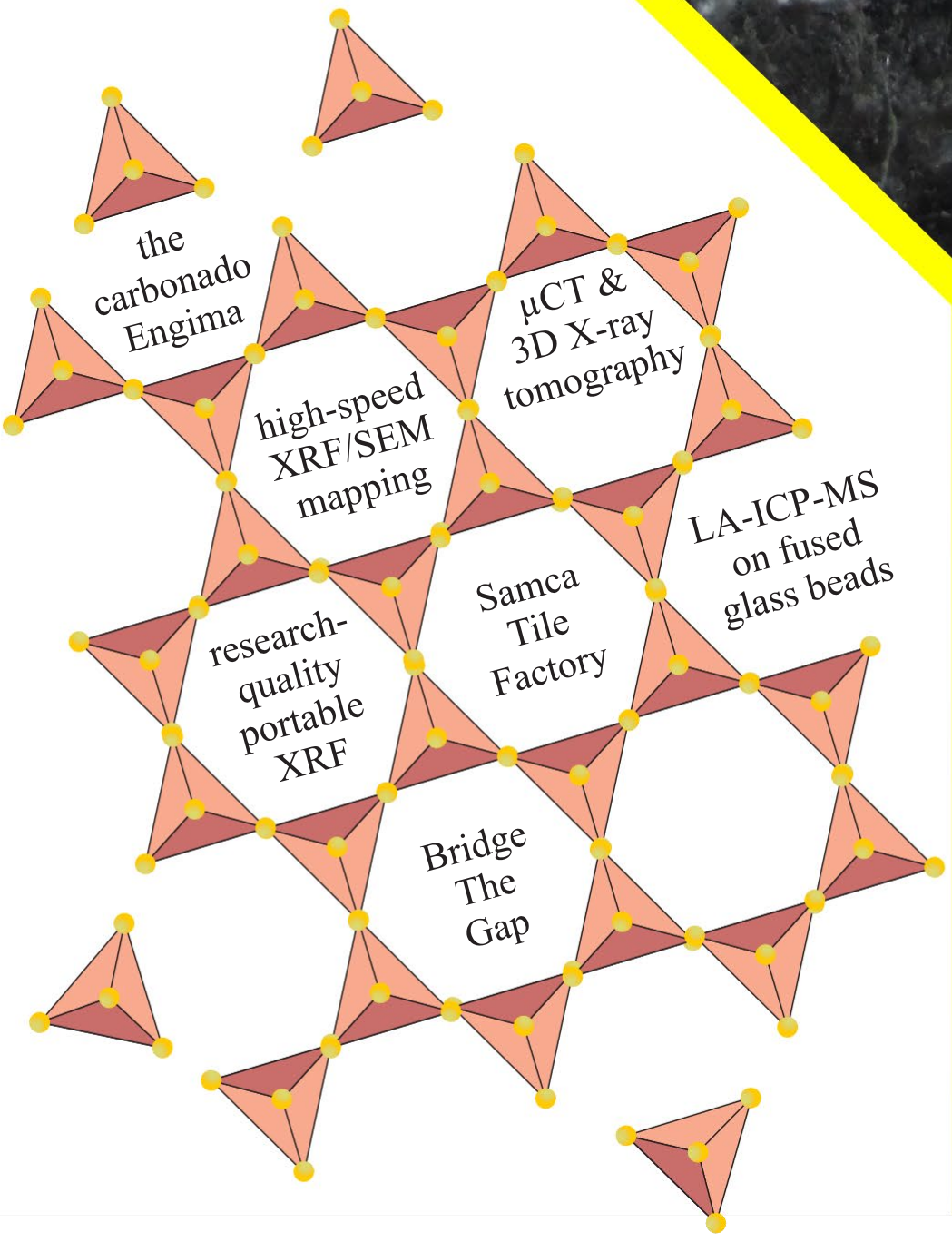

The GEODE

Minsa Newsletter
Volume 9
No. 1
March 2022

MINSA
Mineralogical Association of South Africa
A division of the GSSA

website: www.gssa.org.za/Minsa
e-mail: Minsa@gssa.org.za

the Geode
the Geode
NEWSLETTER
Volume 9 No. 1
March 2022

2022: IMA's Year of Mineralogy

Contents

Next issue theme:

Analytical data sources for you a nd your students (see pg. 22)

Forthcoming Events & Attractions

These events are still missing dates, as a consequence of lockdown logistics: Minsa will let you know! Watch for e-mailed announcements.

- Bulk commodities talk (TBA)
- Wirsam Visit (TBA)
- SAIMM current president Isabel Geldenhuys will present a talk on slag glass (TBA)
- BTG Talk (August 2022)
- R512 Dolomite Pub Crawl (Late 2022 - Lesedi Cultural Village, Lazy Lizard Brewhouse, L'Atmosphere Bistro, Nikita Restaurant Motel, Blue Night Revue Bar, Gem of the Bushveld Sportsbar).

(TBA = to be announced)

The Editor's Site

Welcome to the first issue of the Minsa Geode for 2022. As noted in our subheader above, that warm tingly feeling you've been noticing since January is probably because 2022 is indeed the International Mineralogical Association's official "Year of Mineralogy". Either that or it's time for your annual check-up. It begs the question, does the IMA have years for other things; was 2021 the IMA's year of poetry, for example? Regardless, according to the IMA Mineralogy 2022 (this year's annual meeting in Lyon, France) website, "Mineralogy 2022 is a global initiative to highlight the importance of mineralogy in our everyday lives. Mineralogy 2022 will consist of

coordinated activities at the regional, national, and international levels. These activities will emphasise the importance of mineralogy as basic fundamental science." So, get busy, people. Mineralogy, mineralogy, mineralogy.

The Editor, channelling Major General Ambrose Burnside.

In this issue, our featured theme is the applications of tried and true analytical technologies in novel and new ways. Accordingly, we feature an article on the other things you can do with glass fusion discs apart from sticking them into an XRF one at a time for major element analyses, like stacking them up and aiming electron beams or lasers at them. We'll read a lot about the use of X-rays; elemental mapping on the SEM from our friends at Bruker, and 3D X-ray imaging from our friends at Zeiss. Willem Kruger shows us what you can accomplish with only a hand-held XRF spectrometer, a lot of patience, resilient squatting muscles, and a good idea; an M.Sc. thesis and a paper in Nature Communications, among other things. We'll also read about the long-awaited (presumably; long-postponed, certainly) Minsa outing to the Samca Tile Factory earlier in March. Elsewhere, Christian Koeberl and Uwe Reimold enlighten us on the enigma of the carbonado diamond, in light of the recent sale at auction of the diamond formerly known as the Enigma. In addition, I fill up some space on the general theme of repurposed analytical tools by speculating on the implications of the recent (but fast-disappearing, thankfully, as the need appears to be receding) widespread use of external thermometers as health monitors. We wrap up with Bruce's photo essay on Smithsonite (not named after The Smiths), and this issue's mineralogical crossword, featuring the theme of "polymorphs" (no, not the squiggly things that grow up to be frogs).

Finally, the Editor notes a spelling error in the last issue of the Geode, where on page 9, reference was made (and a photo offered) of the picturesque Karoo burg of Graaff-Reinet, misspelled as Graaf Reinet. In fact, the town name is a hybrid of the names of the then-governor of the Cape Colony (in the late 1700's), Cornelis Jacob van de Graaff, and his wife, Reinet (presumably). It is not, as I mistakenly implied, named for a Count (hence the title Graaf or Graf, in the Germanic languages) named Reinet.

The airship Graf Zeppelin, named for the Count (Graf) Ferdinand von Zeppelin, from Wikipedia, photographed in 1930. Let's see the IMA get a Zeppelin into its newsletter.

We regret the error.

And that's the perspective from the Editor's site.

Steve Prevec

From the Chair

Welcome to the first Geode for 2022! We all made it through to the end of 2021 and another Covid wave to unfortunately be met by geopolitical instability which has and is continuing to cause massive human suffering. I hope and believe that the human spirit, better leadership, and better ideas will eventually prevail.

Luckily, we have a great Geode ready to temporarily take the mind off other things with the exciting theme of "New takes on old analytical tools". Contributions include pieces on LA ICP-MS, XRF and microCT imaging. Furthermore, there are also contributions on gems and minerals that include the Carbonado diamond and smithsonite (my favourite mineral name by the way). As always, I am very thankful to all the contributors

who have made our themed Geodes so successful for more than a year now.

Bertus Smith

Chair, 2021-22 Minsa Executive Committee.

With regards to recent Minsa activities, nine Minsa members visited the SAMCA Wall Tile Factory in Hammanskraal on 12 March 2022. Please also make sure to be on the lookout for upcoming Minsa activities which include a visit to Wirsam Scientific as well as a talk on bulk commodities processing. We are hoping these will take place in the first half of the year. We are also working towards organizing some interesting talks and excursions for the second half of the year.

Thank you as always to Steve Prevec for the stellar job he does in compiling and editing the Geode and thank you to all for reading the Geode and keeping up to date on Minsa activities. Do not hesitate to write to us to give feedback on this issue of the Geode and what you would like to see added or improved. Stay happy and safe everyone!

Kind regards,

Bertus Smith

Minsa Activities

5th Annual Southern African Mineral Symposium

Please note that the 5th Annual Southern African Mineral Symposium, originally scheduled for November 2021, is back on in Nov. 2022. For more information, please contact Igor Tonžetić at the Minsa address provided in the advert found in the adjacent pages in this issue.

Minsa visit the Samca Wall Tile Factory

Minsa had the privilege of visiting the Samca Wall Tile factory in Hammanskraal on the 12th March 2022. Mr Hendrikus Nel, the manager, hosted the visit. There were 9 participants in the tour, 5 of whom were Minsa members.

Samca Wall Tile factory forms part of the Ceramics Industries group who manufacture ceramic tiles and bathroom-ware. The Group comprises five tile factories, one bathroom-ware factory and one acrylic bath factory, all based in South Africa, as well as a tile factory in Australia.

Samca Wall Tile is the only factory in the group exclusively geared towards manufacturing wall tiles. Situated in Hammanskraal, the factory produces monocotura (single fired) wall tiles in six different sizes in a highly automated production line. The majority of the products are finished using the latest inkjet technology in the designs, which ensures high definition within the patterns. This factory also focuses on wall-floor combination designs, mainly for bathrooms.

There are two factories in the area; one focussing on floor tiles and another on wall tiles. Minsa members visited the wall tile factory. Minsa members were met at the factory gate and after completing COVID protocols and breathalyser tests, received ear plugs and proceeded to the boardroom where Mr Nel described the entire manufacturing process in a very informative session. He answered our many questions in detail and with a good sense of humour.

The actual plant tour was fascinating – it lasted more than an hour and was very interactive, there were even opportunities to collect some samples along the way. Samca Wall Tile factory has an example of each tile ever produced in the plant! If a tile is out of production, a special production rerun can be undertaken, provided that at least 15 000m^2 of tiling are requested.

Mr Nel showed us aspects of the entire process and again attempted to answer our many queries which arose along the way, despite the noise level in the plant. We concluded the visit with another discussion in a meeting room in the plant. We were able to remove our earplugs and consolidate all the information and final queries which we had.

The figure below shows the process in brief, from milling and blending the raw materials, through pressing and firing the tiles to the final packaging stage.

Some statistics for the production enthusiast:

- There are four different types of tile finishes - matte, shiny, translucent and coloured.
- Any design can be printed onto a tile, supplemented by silica glass for that special effect; about 2000-3000 m^2 of these tiles are sold in a year.
- Tile sizes are (200 X 200) mm, (200 X 300) mm, (250 X 400) mm, (200 X 500) mm, (300 X 600) mm and (265 X 800) mm.
- 22 000 m^2 of tiling produced per day.
- 10 000 tonnes of clay/day.
- 2000 tonnes of silica/day.
- Design shows assist the tile manufacturer to keep track of market trends.
- New tile designs are showcased for buyers.

Some useful links with for those who have FOMO:

https://www.ceramic.co.za/factories/samca-wall-tile-factory)

Grinding media:
http://www.industriebitossi.com/lang1/alumina_grinding_media.html

https://www.youtube.com/c/CeramicIndustries1976/videos

https://www.ceramic.co.za/downloads

Contributed by M. Safi

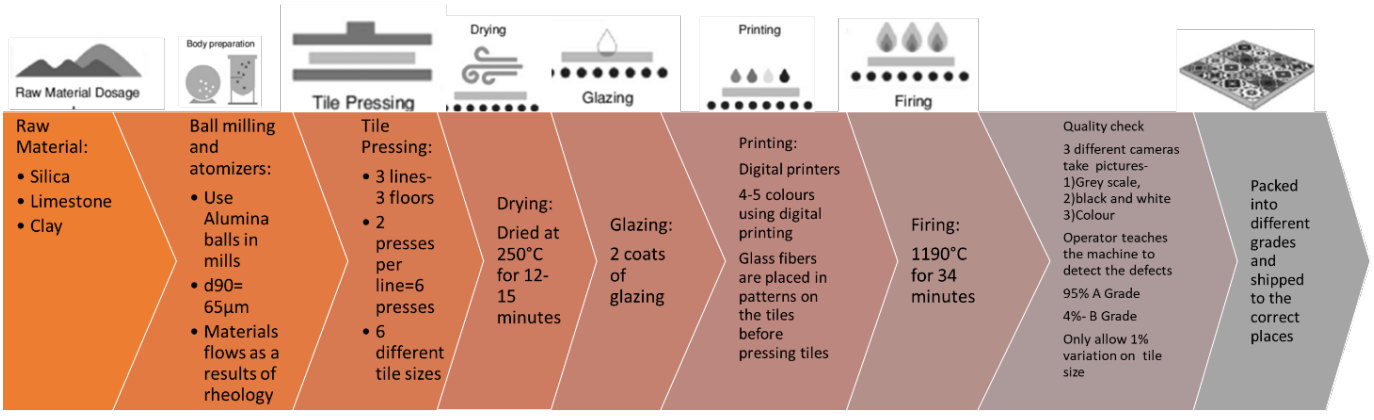

5TH SOUTHERN AFRICAN MINERAL SYMPOSIUM 2022

A REVISED SECOND CIRCULAR

A one-day symposium highlighting minerals and mineral and gemstone deposits of southern Africa hosted jointly by the Mineralogical Association of South Africa, University of the Witwatersrand and the South African Micromount Society

Important Information

Date: T.B.A. November 2022
Venue: University of the Witwatersrand, Johannesburg
Cost: R175.00 (attendees); R100 (presenters) – Reduced from 1st Call (includes tea/coffee & packed lunch)
Enquiries: Symposium Chairman – Igor Željko Tonžetić: minsa@gssa.org.za

Abstracts Due Date: T.B.A. August-September 2022 (Extended Submission)

The Mineralogical Association of South Africa (MINSA) in conjunction with the South African Micromount Society (SAMS) and the University of the Witwatersrand would like to invite you and all interested parties to submit abstracts/extended abstracts/short communications (for presentation) at the 5th Southern African Minerals Symposium 2022. Please try to keep your abstracts/ extended abstracts/short communications down to 2 pages (Calibri 11, Single Line Spacing). Abstracts/extended abstracts/short communications longer than 4 pages will not be accepted. You are welcome to include images/figures/pictures/photos/diagrams etc in your abstract. You are also welcome to include references. Be sure to include a title, author name, and affiliation/address in your abstract. Accepted abstracts will be published with short biographies.

A poster programme will run concurrently. As such you are also welcome to submit posters for display.

Background to the symposium…

This symposium will be the fifth 'mineral symposium' that has been held in South Africa, albeit not on a very regular basis. The '*1st International Gem & Minerals Symposium'* was organised in September 1975 by the Pretoria Gem & Mineral Club in Pretoria on behalf of the Federation of South African Gem and Mineralogical Societies. Four overseas and three local mineralogists and gemmologists delivered a series of talks over three days and one day was taken up by field trips. The themes of the lectures were focused primarily on overseas minerals, mineral localities and on gemstones.

Seventeen years later! Bruce Cairncross organized and convened the '*First SA Mineral Collectors Symposium'* at the Rand Afrikaans University in Johannesburg in September 1992. This concentrated more on local content than the first symposium held in Pretoria, which had a distinct international flavour. This took place over a week-end with thirteen local experts presenting talks on various aspects of minerals, mineral localities, mineral identification, analytical techniques and gemstones. After a day and a half of talks, delegates then visited some of the local collectors in the Johannesburg-Pretoria area to view their collections.

Eighteen years later, in 2010 the '*3rd Southern African Mineral Symposium'* was held at the Council for Geoscience in Pretoria. Jointly organised by some members of the Witwatersrand Gem and Mineral Club and the South African Micromount Society, this one-day event showcased local experts and specialists (both amateur and professional) in mineralogy, gemmology, mineral collecting and related topics presenting a wide ranging series of talks and poster displays on the region's minerals and gemstones. The symposium was a tremendous success, with over 100 participants, 14 speakers along with 9 poster presentations.

Similarly, and heralding on from the success of the previous symposium the 2012 symposium was held at the Council for Geoscience in Pretoria and attracted 12 speakers with over 100 delegates in attendance. Topics included: the Phalaborwa Complex, Okiep Copper District, the industrial archaeology of silver in the Pretoria region, microminerals of the Bushveld Complex, FOSAGAMS mineral excursions, the Museum Africa minerals collection, mineral connoisseurship, detrital rutile, diamond morphology, tanzanite, meteorites, the Kalahari Manganese Field and the Rosh Pinah Pb-Zn Mine.

The purpose of the 2022 symposium (as with previous symposiums), is twofold. Firstly, to get together the 'professionals' and the 'amateurs' who are experts in their respective fields and to have stimulating discussions on minerals, gems and related topics. Secondly, the symposium acts as a vehicle for promoting and highlighting minerals, mineral heritage, mineral collecting and mineral preservation in our region. It is therefore envisaged to use the success of the current symposium, and the previous ones, to have these on a more regular basis.

Articles

The March issue theme: New takes on old analytical tools.

In December we invited our readers to share insights into new or novel applications of traditional analytical tools for the modern geologist. In our selection, the management and measurement of X-rays appears to be the basis for the most in-demand and utilitarian tools from research to exploration to industry. We feature four submissions here, for your edification and enjoyment.

- Major elements by LA-ICP-MS (Steve Prevec)
- High-speed elemental mapping by dual source X-ray and electron SEM (Andrew Menzies & Stephan Boehm)
- Big science with a small XRF (Willem Kruger)
- 3D X-ray microscope and microCT imaging (Eddy Hill)

Analysing major and trace elements: traditional XRF versus LA-ICP-MS

or

What else can you do with fused glass beads?

The Editor lines up a penalty kick.

Steve Prevec
Dept of Geology, Rhodes University
Makhanda, RSA

Traditional whole rock (or bulk rock, if you prefer) analysis of the major and trace elements has been conducted for decades using XRF spectrometers. The major elements (those elements present in concentrations of their oxides on the order of 1.0 wt.% or higher, as well as a few of their friends (minor elements) present at 1.0 to 0.1 wt. % (1000 ppm) are typically analysed by X-ray bombardment of a fused glass bead, and the subsequent detection and measurement of the resultant secondary X-ray emissions. The bead is manufactured by mixing a precisely known weight of finely-ground (>400 mesh particle size, to facilitate mixing and melting) with typically about ten times more flux, normally an oxide compound of low-melting temperature elements such as Li and B. This mixing has the effect of lowering the melting temperature of the rock to manageable (Bunsen Burner-friendly) temperatures and producing a melt which is of sufficiently low viscosity that it can be relatively effectively homogenized (normally by swirling it in a platinum crucible created for such a purpose), and can be poured out without sticking to the crucible or beading up and leaving material behind. The melt is then poured into a platinum mould, where it cools (slowly, to avoid cracking) to a solid glass disc.

> XRF, or X-ray fluorescence spectroscopy, involves the production of primary X-rays from an excited source (usually tungsten, but Mo and Cu are also used), directed into a solid sample, from which low-energy secondary X-rays are emitted as a consequence of knocking electrons out of their normal orbitals, causing them to scramble for the lowest vacant orbitals like subatomic musical chairs.

This 10:1 dilution has the effect of making it very difficult to then also analyse trace elements in the same disc, as the effective detection limit of XRF spectrometers is on the order of say, 10 to 2 ppm, depending on the element. By diluting the sample by a factor of 10, the detection limit is effectively raised by a factor of 10 (so now 100 to 20 ppm). For this reason, trace elements such as the transition metals, and a few of the high field strength elements (such as Zr, and maybe Nb and Ce if the rock is not too mafic and HFSE-poor) are analysed using pressed powder pellets. For these, sample homogeneity is compromised for concentration, so several grams of the same finely-ground (which now serves to minimise crystal structural effects) sample powder are mixed with an organic binding agent, packed into a mould (of which there are various designs; I used aluminium cylindrical cups as a postgraduate student (although since that was in Canada, they were in fact made of aluminum, without the surplus "I"). The mould and powder and

then compressed in a manually-operated 10 ton manual hydraulic press which flattens them into a compact disc (but not the kind that plays music), just as satisfying as (but much less hazardous than) putting pennies on the train tracks before the locomotive comes by.

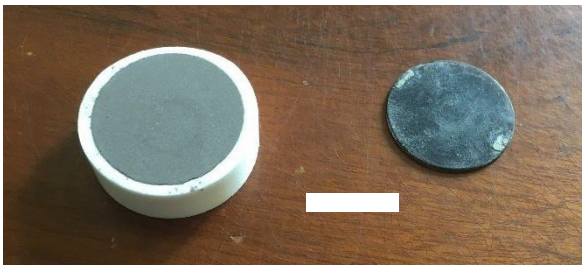

A pressed powder pellet (left), and a fused glass disc (right). Photo by the author. Scale bar ~ 1 cm.

From the 1970s onwards 'til today, the ol' XRF is still a quick, reliable and affordable tool for major and minor elements in 'normal rocks'. Up until the advent of ICP and then ICP-MS in the 1990s, it was also the best tool for most trace elements of interest. If you wanted the rare earths, or gold and its platiniferous neighbours, you had to employ more labour-intensive preconcentration methods such as chemical chromatography or fire-assay (respectively), and then use instrumental neutron activation, requiring the aid of a small nuclear reactor. The ICP-MS has made that semi-redundant for most geological users (although if you want PGE abundances in unmineralized rocks, you are still pushing your luck even with fire assay and ICP-MS; I've got the invoices and the accompanying printouts festooned with bdl (below detection limit) to prove it).

LA-ICP-MS stands for laser-ablation inductively-coupled mass spectrometry. This involves the use of a laser to ionize a very specific volume of polished surface of target material, which is then whisked away by an ionized gas cloud into a noble gas-based plasma, at ca. 10,000K (or only 9727°C), which sends it into a mass spectro-meter as charged ions and a few molecules. There the ions are separated according to mass, detected as electronic signals and converted into a measureable quantity.

However, in the last two decades, creative thinkers have recognized that although fused beads were too dilute for the XRF to make effective use of for elements much below 100 ppm, there were other options. Some experimented with more concentrated rock/flux mixtures, daring to explore the possibilities of 5:1 and even 2:1 (although this was found to be too extreme) flux:sample ratios (Mori and Mashima, 2005). This heightened the risks noted above, but improved the detection limits by a factor of two (implicitly). However, by using an ICP-MS, with a detection limit in the parts per billion range, the potential for glass bead analyses is greatly enhanced. The sample dilution of normal fused beads at 10:1 is comparable, or is probably an improvement on the dilution normally experienced in dissolving a few hundred milligrams of powder in the appropriate acids and eventually producing a dilute solution of modestly concentrated nitric acid to be aspirated into the plasma jet of an ICP spectrometer.

A study by Ganev (2013) tested the use of LA-ICP-MS on powder pellets (too inhomogeneous), fused sample powders (at 1600°C, which was technically inconvenient and expensive), and finally on fluxed sample glass beads (just right!). This study found excellent agreement between XRF and the LA-ICP-MS results. Kurosawa *et al.* (2006) found similarly good major element correspondence, and also good correspondence between trace elements at ppm-levels analysed by LA-ICP-MS as compared to those obtained by normal dissolution and nebulized (*i.e.*, sputtered in as a liquid) ICP-MS, apart from Cu, which tended to want to stay behind in the platinum crucible. Ganev (2013) used carbon crucibles, which might alleviate that problem. Kim *et al.* (2015) demonstrated that for the same range as that for which XRF is normally applied (*i.e.*, down to ca. 10 ppm), a comparable level of reproducibility (ca. ± 10%) can be achieved over a wide range of trace elements in fused glass beads. Even more recently, while we were feeling sorry for ourselves in lockdown, Leitzke *et al.* (2021) brought good cheer to readers of the Brazilian Journal of Geology, to whom they showed that even for the low concentration incompatible high field strength elements in mafic and ultramafic rock standards, good data can be acquired, although they still found that the siderophile elements tended to get distracted by the platinum crucibles used for the fusions. This means

that properly prepared and standardized and calibrated, fused beads alone can be used as a reasonably effective one-stop-shop for major and trace elements for research purposes.

The efficiency of the LA-ICP-MS technique on fused beads can be enhanced by the device of, rather than analysing individual beads as distinct samples, using sets of fused discs that are stacked up, glued together and mounted in epoxy, then polished to normal EPMA-SEM requirements and sent to the LA-ICP-MS lab to zap the discs in cross section, one after another. Don't forget to write down the sample numbers of the discs before you stack them up and glue them together. This method is also used for major element analyses conducted by EPMA (electron microprobe). I don't have a reference for this technique, but I heard tell of it ten year ago in Canada, from a Swiss feller who had heard about it in Queensland, but was on his way to Ireland at the time. Yes, it was a pers. comm. (2010) from Balz Kamber, but I can't find an actual published account of this, and I couldn't raise him by e-mail. Take it or leave it.

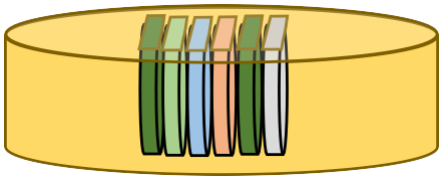

Artist's conception of polished stack of fusions in an epoxy mount.

References

Ganev, V. (2013) Quantitative LA-ICP-MS analysis of major elements in lithium tetraborate fused silicate rock beads. Proceedings of the Bulgarian Academy of Sciences, vol. 66: 1595-1602.

Kim, M.J., Kim, T., Park, K.-H., Lee, Y.J., Yang, Y.-S. & Moon, J. (2015) Evaluation of LA-ICP-MS whole rock trace element analysis using fused glass bead of silicate rocks. The Journal of the Petrological Society of Korea, vol. 24: 141-147.

Kurosawa, M., Shima, K., Ishii, S. & Sasa, K. (2006) Trace element analysis of fused whole-rock glasses by laser ablation-ICP-MS and PIXE. Geostandards and Geoanalytical Research, vol. 30: 17-30.

Leitzke, F.P., Wegner, A.C., Porcher, C.C., Malüe, N.I., Berndt, V.J., Klemme, S. & Conceição, R.V. (2021) Whole-rock trace element analyses via LA-ICP-MS in L glasses produced by sodium borate flux fusion. Brazilian Journal of Geology, 51: e20200057.

Mori, Y. & Mashima, H. (2005) X-ray fluorescence analysis of major and trace elements in silicate rocks using 1:5 dilution glass beads. Bulletin of the Kitakyushu Museum of Natural History & Human History, Ser. A, vol. 3: 1-12.

Dual source X-ray and electron SEM system: High-speed elemental mapping of an epithermal gold-bearing sample from Karangahake, New Zealand

Andrew H. Menzies & Stephan Boehm
Bruker Nano Analytics GmbH, Berlin; Germany

Micro-X-ray fluorescence spectroscopy [XRF] is a long known and complementary analytical technique to e-beam Energy Dispersive Spectroscopy [EDS] for the characterization of the elemental composition within samples. The Bruker XTrace X-ray source enables the XRF technique to be utilized on a Scanning Electron Microscope [SEM]. Micro-XRF excitation analysis is also a small area (volume) technique ideal for low kV or beam sensitive samples as there are no charging effects (*i.e.*, minimal sample preparation), the advantages of which include higher sensitivity for the detection of trace elements, higher energy X-ray line excitation (full spectrum range up to 40 keV), as well as information from greater depth within the sample. The availability of modern X-ray polycapillary optics yields a X-rays focus spot size of less than 30 µm, all contained in an X-ray source that can be mounted on a SEM port. X-ray energy detection uses the existing Bruker EDS detector on the SEM. Accordingly, the SEM system will subsequently have dual source potential, *i.e.*, both an electron and an X-ray source (Figure 1), which together offers new possibilities for material characterization.

The SEM user can operate a micro-XRF system using similar parameters as an e-beam system, yielding results comparable with traditional SEM-EDS analysis,

whilst obtaining additional information from the X-ray source sample interaction.

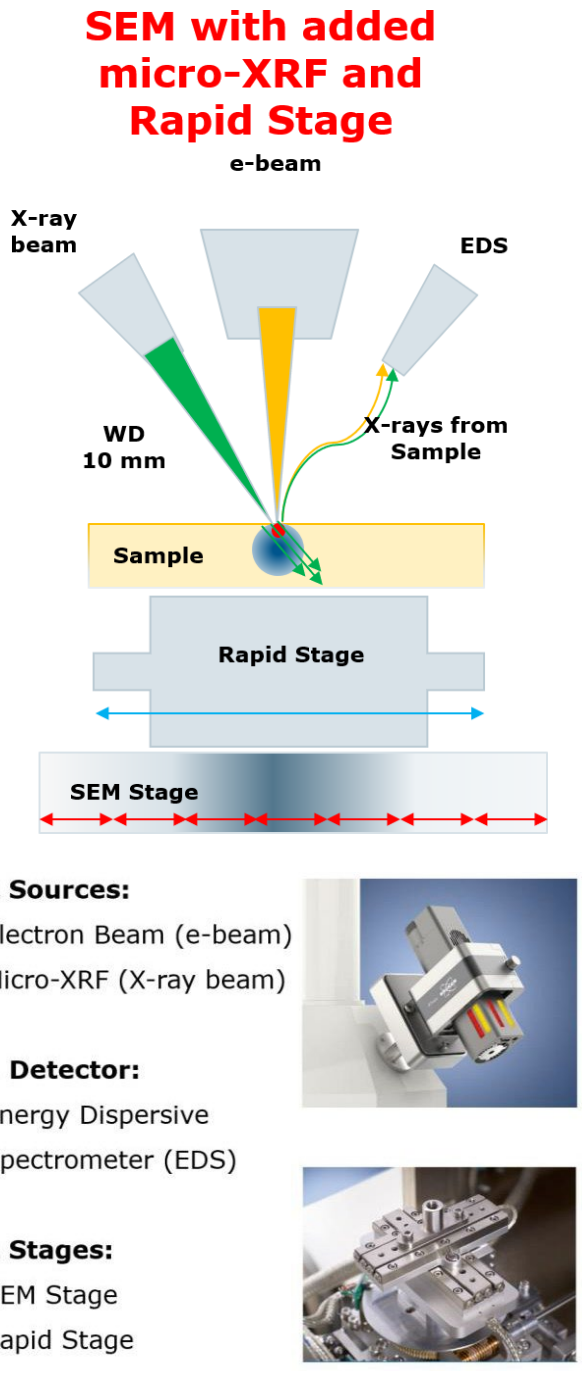

Figure 1. *The Micro-XRF works with a fixed beam and cannot raster like an e-beam. Therefore, a special stage (Rapid Stage) has been developed for high-speed element distribution measurements with X-ray excitation. This stage is mounted on top of the existing SEM stage and can be easily removed when it is not required.*

Electron excitation has a higher excitation efficiency for light elements (e.g., Na, Mg, Al, Si), and it is possible to perform measurements down to Boron. X-ray excitation efficiency is better for heavy elements (e.g., Cr, Mn, Fe, Co) and allows the detection of trace concentrations down to 10 ppm for certain elements. The larger depth of X-ray excitation allows a deeper look inside the sample, allowing the characterization of relatively thick layers or even of multilayer systems starting from 1nm and ranging to 40 µm, which is not possible with electron excitation. Micro-XRF works with a fixed X-ray beam, consequently, X-ray elemental distribution maps must be acquired via stage movement. Developments of adding a piezo-based stage (Rapid Stage) mounted on top of the SEM stage enables high-speed elemental X-ray mapping over large areas (Figure 1), thus making it suitable for the analysis of larger samples (i.e., centimeter scale) that traditionally analysed in an SEM. Seamlessly integrated into Bruker ESPRIT software suite, it even allows for simultaneous electron and micro-XRF acquisition, incorporating light element spectral data as well as trace element and / or higher energy X-ray data. Sample preparation requirements are minimal for micro-XRF analysis and thus a wide range of sample types can be analyzed (e.g no carbon coating required; no high-quality polished surface required; low vacuum). Applications include economic geology, petrology, mining, mineral processing, forensics, environmental and archaeology, amongst others.

In this application relevant to the field of Geology, Exploration, Mining and Metallurgy, the objective is to determine elemental and mineralogical information about the sample to aid in understanding the geological processes and potential economic deposit genesis as well as mining, metallurgical and mineral processing considerations. This demonstrates the potential when utilizing the benefits of a combined electron and X-ray excitation system on a SEM. The selected sample is from a gold-bearing epithermal deposit (Karangahake) in New Zealand. Figure 2 is an image of the gold-bearing sample to be analyzed. The table in Figure 2 shows the relevant minerals and elements of interest. Figure 3 is a mosaic map of the elements of interest and the selected analytical

conditions as measured using the micro-XRF source. In addition, in this sample it is possible to detect trace elements such as the K-Lines for Se, Ag, Cd, and Sb that are not usually detectable by e-beam EDS as the concentrations are too low and/or the relevant element energy line is too high, and thus understand their distribution and mineralogical and textural relationships.

Mineral	Formula
Native Gold	Au
Native Silver	Ag
Sulphides	
Pyrite	FeS_2
Chalcopyrite	$CuFeS_2$
Galena	PbS
Sphalerite	ZnS
Gangue Mineralogy	
Quartz	SiO_2
Adularia	$KAlSi_3O_8$

Figure 2. *Gold-bearing epithermal sample from the Karangahake deposit, New Zealand. The sample is approximately 5 cm in width. The inset table lists the relevant minerals and elements of interest. The sample is carbon coated as both X-ray and electron analyses will be performed.*

As can be seen in Figure 3, the micro-XRF hypermaps successfully identify the presence and location of gold (Au) and silver (Ag) bearing grains within the sample. In addition, it is possible to ascertain that these gold grains are primarily native gold or electrum. This large area map was achieved in 94 minutes. Furthermore, there are known peak overlaps for the various gold peaks, and thus an intensity map of a single Au element line might lead to misinterpretation. For example, the gold L-α line has an energy of 9.704 keV, which overlaps with Zn K-β (9.569 keV) and W L-β (9.682 keV), both of which occur in Au-bearing deposits. Thus, to confirm the presence of Au, the information must be correctly deconvoluted, and the presence of all the Au element lines should be confirmed. Figures 4 and 5 clearly demonstrate that gold is present in this sample using the functionality of the Maximum Pixel Spectrum, and interactively selecting individual pixels and groups of pixels within the hypermap.

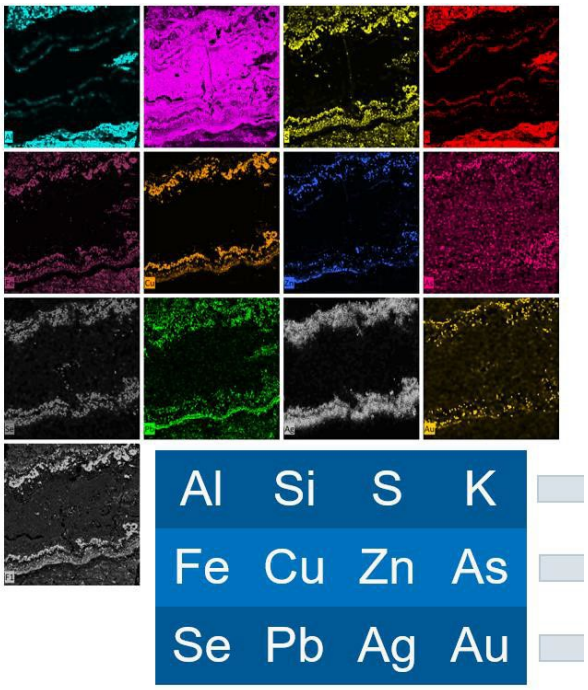

Beam:	X-ray
High Voltage:	50 kV
Anode Current:	600 µA
Analytical Spacing:	**100 µm**
Dwell Time:	**32000 µS (32 mS)**
Analytical Area:	4.5 x 4.5 cm
Total Analytical Time:	**94 minutes**
Spot Size:	25 µm
Interaction Depth:	10 – 100 µm

Host Rock Elements: Al, Si, K

Mineralisation: S, Fe, Cu, Zn, As

Economic Mineralistaion: Au, Ag, Se

Figure 3. *Large area X-ray map (45 mm x 45 mm) of an Au-bearing epithermal sample acquired with XTrace (Analytical Parameters: Tube Voltage: Rh at 50 kV; Anode Current: 600 µA; Pixel Spacing: 100 µm; Analytical Time: 94 mins). Elemental Maps as indicated in the blue box at bottom of image. Note the mineralisation, especially Ag and Ag alone as parallel veins.*

(continued on next page)

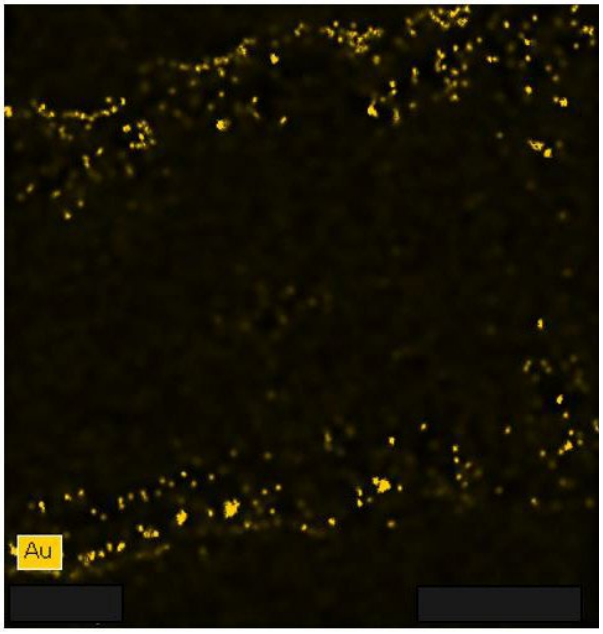

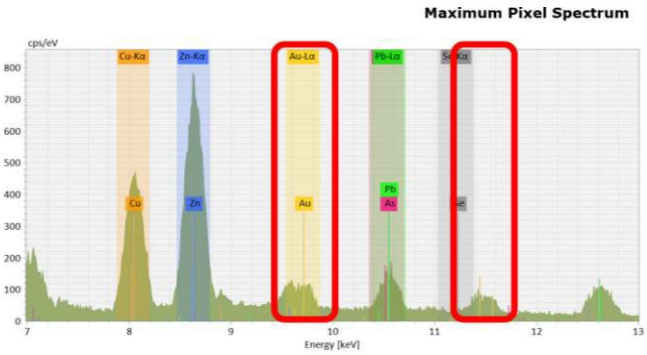

Figure 4. At left, *Au elemental intensity distribution map (Au-Lα energy line 9.7 keV). Deconvolution Applied. Distinct and clear Au-Lα and Au-Lβ X-ray energy Lines are visible in the Maximum Pixel Spectrum and thus the presence of Au in the sample is confirmed. The Maximum Pixel Spectrum shows the maximum intensity measured for each energy channel for the entire map area.*

Now that the presence of gold has been confirmed and the various positions of gold bearing grains identified, it is possible to analyse selected areas using the electron beam to yield higher resolution maps over specific areas. These follow-up analyses can be achieved by switching to e-beam SEM analyses (which requires sample coating and high vacuum) or selecting specific areas in the sample for further sample preparation prior to analysis. In this case the former is preferred, and examples of such maps are shown in Figure 6 and clearly highlight the fine scale relationship between Au and other elements associated with the mineralization such as Zn, Fe, Cu, and Pb. Thus, in the space of one analytical session, the benefits of dual source X-ray and electron SEM system in the analysis a gold-bearing sample were utilized.

Below: Figure 5. *Au Elemental Distribution. (Au-Lα Energy Line 9.7 keV). Deconvolution Applied. Distinct and clear Au-Lα and Au-Lβ X-ray energy Lines are visible in the selected individual and summed pixel points, thus confirming the presence of Au in the sample*.

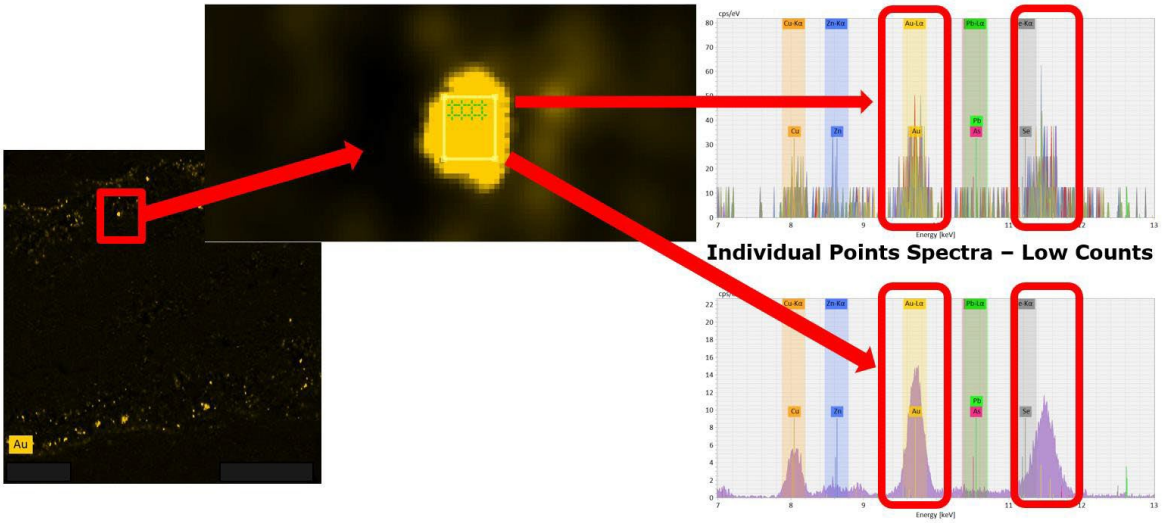

Distinct and clear Au-Lα and Au-Lβ X-ray energy Lines.

Summed points within Grain – High Counts, clear and confirmed elemental peaks

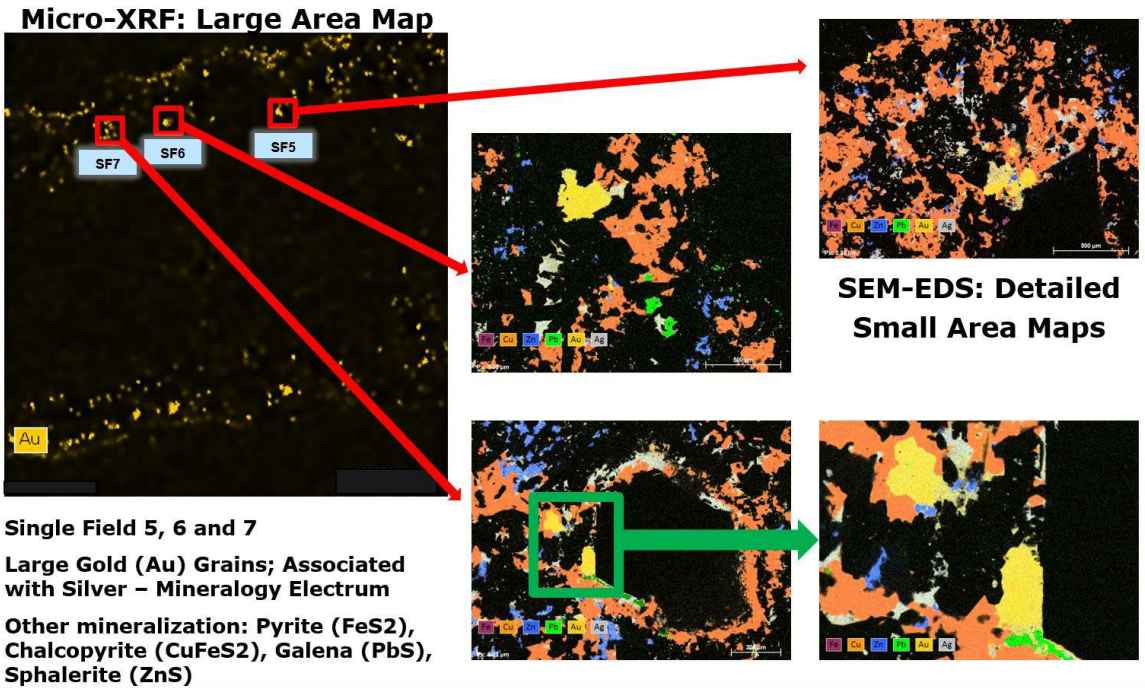

Figure 6. *Electron beam analysis of selected areas where gold grains are known to be present resulting in a high resolution (1 µm or less) element intensity maps enabling the identification and relationships between the Au-grains and various sulphides.*

Application of the hand-held XRF in the geosciences

Willem Kruger
School of Geoscience
University of the Witwatersrand

About fifty years after Wilhelm Roentgen's accidental discovery of X-rays, X-ray florescence spectroscopy was established as a practical method to chemically analyse materials towards the end of the 1940s. It took another 34 years for the method to escape the confines of the laboratory with the introduction of the first "portable" XRF, that reportedly weighed 31 kg in 1982. Its primary use was the investigation of radioactive waste and the detection of uranium in potentially contaminated soils. Continued improvements in this technology eventually led to the creation of the 7 kg, hand-held XRF spectrometer (hXRF): the Niton XL-309, introduced in 1994. While the lightest element it could detect was titanium, further improvements allow modern instruments to analyse much lighter elements, potentially all the way down to Mg.

In comparison to laboratory analysis, these portable instruments have some major advantages. Analysis is fast, non-destructive, and can be carried out directly on field outcrops or drill core. Very little sample preparation may be required, and the method can produce enormous quantities of geochemical data at a tiny fraction of the cost. However, these advantages are also met with some significant drawbacks. While the lower power output of these instruments (typically below 4W compared to as much as 100W for laboratory instruments) make them safe to use, this also gives a weaker signal, resulting in greater analytical error, especially for the lighter elements. Therefore, while some light elements (like Mg) can be detected by the instrument, the results are generally less reliable than for heavier elements, while other geologically important elements (such as Na) are typically not measured at all (Young *et al.*, 2016). Direct use of hXRF on

field outcrops present some additional challenges. Since the instrument only analyses a very thin surface layer of the exposed material, weathering and/or staining of the surface can lead to extremely variable results. For optimum results, the surface analysed should also be perfectly flat, otherwise the actual concentrations of elements present may be dramatically underestimated. If the operator slips or makes small movements with the instrument during the analysis, this will also further decrease the analytical precision, making the instrument susceptible to user error.

However, these challenges have certainly not stopped some geoscientists from making use of the hXRF as an invaluable field companion. While it may be difficult to obtain quantitative data from the instrument from field outcrops, preliminary analysis of rocks in the field may aid for better sample selection, reducing laboratory analytical costs and potentially also limiting future trips to the site under investigation (Young et al., 2016). Recent work on massive magnetitite layers from South Africa's Bushveld Complex, the largest layered igneous intrusion on Earth, have shown just how remarkable the use of the hXRF can be, and how certain techniques can be employed to overcome some of the limitations associated with the instrument. The chemistry of magnetite is extraordinary as it can provide some of the best insights into magma chamber processes compared to just about any other mineral (Cawthorn and McCarthy, 1980). This is because of magnetite's great affinity for chromium. When magnetite crystallizes from magma, it will quickly use the chromium available to it in the surrounding melt to help build its crystal structure. However, chromium typically occurs in very low concentrations in magma, which means that all available chromium in the melt will be rapidly consumed when a magnetitite layer is forming. The process results in extremely steep Cr gradients in the rock, up to several 1000 ppm across just a few cm. Because these gradients are so steep, hXRF appeared to be the perfect tool to map out the distribution of Cr within a single layer of magnetitite, as the distribution patterns would still be visible despite the slightly larger analytical error associated with the instrument. The Main Magnetite Layer in the Magnet Heights locality of the Eastern Bushveld Complex was targeted for this study, where very clean exposures of the layer is present in a stream section. However, since the surface of the magnetitite layer is irregular, the degree of contact varies from one analysis point to the next, making it very difficult to obtain comparable results. Thankfully, a solution to problem lay within the geochemistry of the magnetitite layer itself. While V is also favourably incorporated into magnetite during crystallization, it is far less compatible than Cr, and it has a much more constant concentration throughout the magnetitite layer.

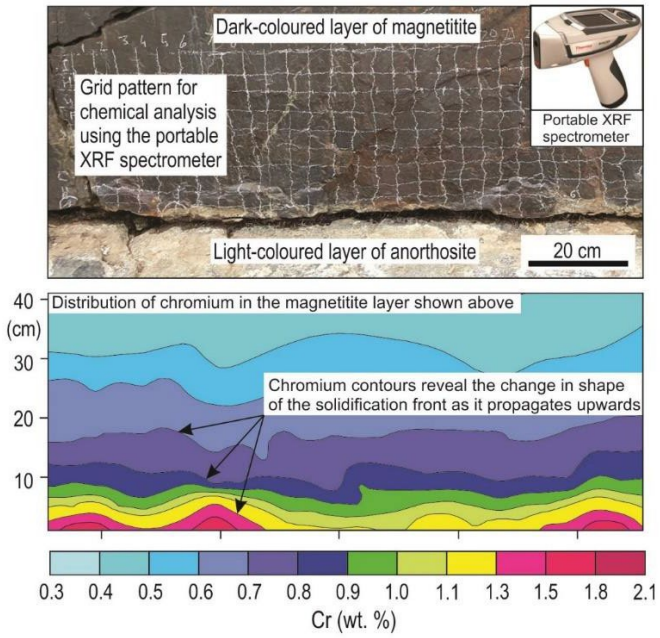

Figure 1. *The layer of magnetitite that was analysed using a Niton XL3t handheld XRF spectrometer. The magnetitite is situated atop a layer of anorthosite. The geochemical map that was produced based on the distribution of Cr in the layer reveals the presence of a fossilized solidification front that was chemically preserved as the magnetitite layer grew upwards. Modified from Kruger and Latypov (2020).*

Despite the fact that the irregular surface contacts delivered variable elemental concentrations, the ratio of the elements were still being reported correctly. It was thus possible to use Cr/V ratios of the magnetitite layer obtained with the hXRF and multiplying it by the known V concentration of the rock to obtain true Cr concentrations that are comparable with in-house XRF analysis of magnetitite. The method revealed beautiful chemical patterns within the magnetitite layer based on hundreds of analysis points, all obtained within less than a day. The shape of the Cr contours were interpreted as revealing the step-wise propagation of a fossilized solidification front more than 2 billion years old (Kruger and Latypov, 2020; 2021).

The author in action. Photo taken by Mr Merrily Tau, provided by W. Kruger

References

Cawthorn, R.G. and McCarthy, T.S. (1980) Variations in the Cr content of magnetite from the Upper Zone of the Bushveld Complex – evidence of heterogeneity and convection currents in magma chambers. Earth and Planetary Science Letters, 46, 335-343.

Kruger, W and Latypov, R. (2020) Fossilized solidification fronts in the Bushveld Complex argue for liquid dominated system. Nature Communications, https://doi.org/10.1038/s41467-020-16723-6.

Kruger, W. and Latypov, R. (2021) Magmatic karst reveals dynamics of crystallization and differentiation in basaltic magma chambers. Scientific Reports, https://doi.org/10.1038/s41598-021-86724-y.

Young, K.E., Evans, C.A., Hodges, K., Bleacher, J.E. & Graff, T.G. (2016) A review of the handheld X-ray fluorescence spectrometer as a tool for field geologic investigations on Earth and in planetary surface exploration. Applied Geochemistry, 72, 77-87.

Whole-particle Liberation Studies: ZEISS Mineralogic 3D

Eddy Hill
Carl Zeiss Microscopy Ltd, Cambourne, UK

Light microscopes (LM) and scanning electron microscopes (SEM) are routinely used for mineral liberation studies – a measure of how accessible minerals are to the recovery process, and of the quality of the feed and the subsequent processing. An unavoidable requirement for the analysis is that the sample be prepared in a manner suitable to the microscope in use. Sample preparation is

not simply an inconvenience imposed by lab equipment but is integral to the quality of the results and the inferences we may make. A poorly prepared sample may suffer density stratification, plucking, doming, agglomeration, pitting, insufficient surface exposure, *etc*. As well as these mechanical sample preparation issues, the analysis is limited to the exposed surface of the mineral and therefore influenced by stereological limitations and the assumption that the exposed surface is representative of the entire sample and a valid description of the particles present. All these issues conspire to produce analyses for which the modal mineralogy, grain size, liberation, and associations information are compromised, regardless of whether the analysis is performed on the LM or with automated mineralogy (AM) software on an SEM. Over time, techniques have developed to ensure we present a representative sample for analysis that is devoid of sample preparation artifacts. For example, the addition of graphite to the sample to encourage particle separation and discourage density stratification, and the analyses of sufficient particles to confidently describe a set of average particles and minimize the limitations imposed by stereology (the interpretation of 3D samples based on 2D information). In all, sample preparation is a meticulous and time-consuming activity, taking longer than a day to complete, commencing with the collection of the material to be analyzed and progressing through to the final stages of setting in a resin block, grinding, polishing, and coating with a conductive layer. None of the steps can be circumvented if we are to guarantee trustworthy data. In the following text is a description of paradigm shift in automated mineralogy that overcomes the issues of attempting to understand a 3D world by analyzing it on 2D surfaces.

ZEISS Mineralogic 3D applies 3D X-ray microscopy techniques and deep learning algorithms to execute automated mineralogy analyses in three dimensions (Fig. 1) that provide particle identification, mineral classification, and data outputs including liberation and association measurements. Analyzing in 3D has three immediate benefits:

1. The sample preparation process is greatly simplified;

2. There are no stereological assumptions as every grain is viewed in full;

3. The time to actionable data is greatly reduced.

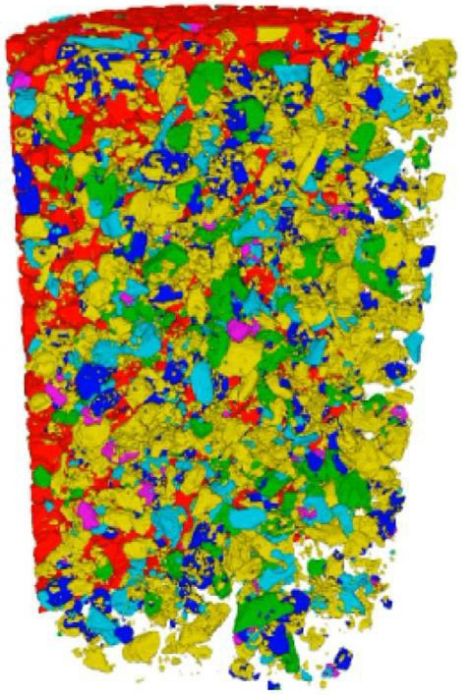

Figure 1. *Analysis of a comminuted ore with the 3D X-ray microscope reveals the true mineral liberation with no mineral hidden by lack of exposure.*

Analytical Considerations

Sample Preparation

Unlike the rigorous sample preparation workflow that must be followed to ensure we obtain valid data from an SEM analysis of a comminuted sample, sample preparation for mineralogic 3D analysis is rather straightforward. All that is needed is a suitable container or tube to hold the sample and a stopper at either end to help keep it in place. A step of complexity has been introduced by the development of a technique that allows for

several samples to be mounted in the same sample carrier (tube) but even with this added labour, this falls far short of the intricacies of graphite addition, mix stirring, setting, grinding, and polishing expected for the SEM analysis. The result is a simplification of the workflow and a time savings of several hours.

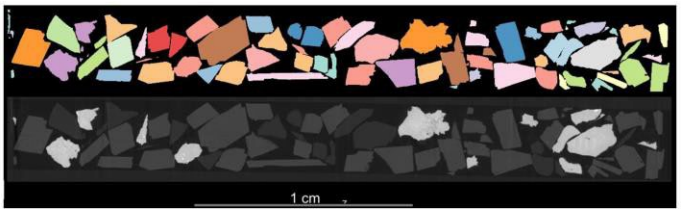

Figure 2. *Longitudinal cross-section of a 3D scan of ground material. The coarseness of the particles provides a clearer example of the ability of the machine learning protocol to automatically identify and separate particles from each other.*

The addition of graphite to the sample acts to both keep particles apart, aiding the assessment of liberation and associations, and to deter gravitational settling in the samples. Since Mineralogic 3D views the entire sample, including minerals locked within the particles, gravitational settling is not a concern. Particle separation is elegantly dealt with by the application of machine learning protocols for segmentation that identify each individual particle as independent from other particles that may be in contact with it (Figure 2).

Mineral Classification and Time to Actionable Data

Making full use of the imaging capability of the X-ray microscopes, enhanced by noise reduction deep learning algorithms, Mineralogic 3D automatically classifies the mineralogy of the sample based on attenuation measurements (Figure 3). The ability to classify the mineralogy in tomographic scans is unique and, when combined with the morphological measurements of the 3D reconstructed entities, allows the calculation of standard mining relevant outputs, for example, morphological parameters, associations, and liberation. The ability to measure not just the surface of particles but their interior mineralogy too adds great value to the data generated. When assessing the value of the data, we must also consider the time lapse between asking a question of the sample and obtaining an answer – if the data is to lead to an action, rather than an understanding, then it must arrive within the opportunity window for which it can be actioned. Next week is too late. Taking full advantage of the simplified sample preparation workflow, Mineralogic 3D delivers actionable data in a fraction of the time required by a metallographic preparation for the SEM.

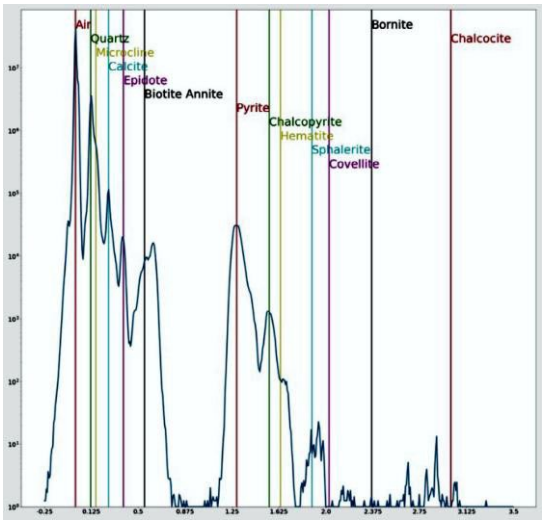

Figure 3. *Mineral classification based on beam attenuation measurements.*

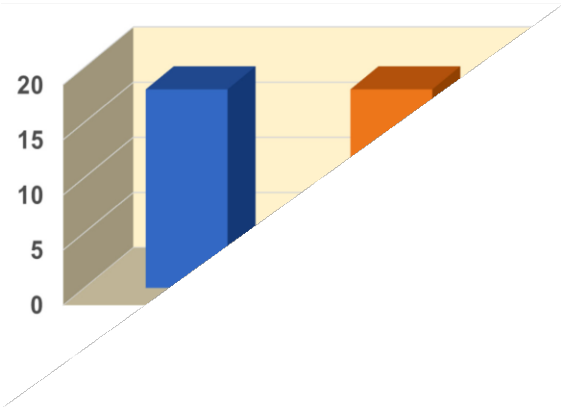

Figure 4. *The simplicity of sample preparation combined with advanced analytical techniques results in a marked time savings in results delivery with Mineralogic 3D.*

ID	Mineral	Volume %	Volume % w/o Porosity	Mass %	Volume (mm3)	Volume w/o Porosity (mm3)	Mass (mg)	Average Grain Mass (mg)
2	Quartz	54.7	54.63	51.9	1.48e+00	1.47e+00	3.9e+00	2.04e-04
3	Microcline	27.67	27.7	25.36	7.47e-01	7.47e-01	1.91e+00	6.19e-05
4	Calcite	5.98	6.01	5.81	1.61e-01	1.62e-01	4.37e-01	3.33e-05
5	Epidote	2.91	2.91	3.55	7.86e-02	7.86e-02	2.67e-01	1.12e-04
6	Biotiteannite	3.51	3.51	3.99	9.47e-02	9.46e-02	3.0e-01	2.23e-04
7	Pyrite	4.68	4.69	8.41	1.27e-01	1.27e-01	6.32e-01	8.45e-04
8	Chalcopyrite	0.36	0.36	0.54	9.73e-03	9.73e-03	4.07e-02	1.91e-04
9	Hematite	0.16	0.16	0.3	4.27e-03	4.26e-03	2.26e-02	1.71e-04
10	Sphalerite	0.01	0.01	0.01	2.02e-04	2.02e-04	8.17e-04	3.03e-05
11	Covellite	0.01	0.01	0.01	1.49e-04	1.49e-04	6.98e-04	3.49e-05
12	Bornite	0.01	0.01	0.02	2.89e-04	2.89e-04	1.47e-03	5.08e-05
13	Chalcocite	0.01	0.01	0.03	3.55e-04	3.55e-04	2.0e-03	1.11e-04

Figure 5. *Modal mineralogy based on the volume of the mineralogy.*

Measurements

Immediately at the end of the analysis, Mineralogic 3D reports on modal mineralogy, liberation, associations, particle and grain size, etc. All measurements that are in principle familiar to users of automated mineralogy on the SEM, however, there are some subtle and relevant differences between the two techniques.

Sample exposure

Automated mineralogy on the SEM requires particles to be fixed in resin block that is then ground to expose particle portions, and polished to present a good surface for analysis. Grinding and polishing result in the mechanical alteration of the sample and exposes only a fraction of the particles and mineral grains present. With Mineralogic 3D there is no mechanical alteration of the sample necessary and at any time, and every grain in the sample is visible to the analysis.

Modal mineralogy

Modal mineralogy considers the volume of each phase present in the sample. It need not be exposed on the surface to be accounted for (Figure 5).

Liberation

Liberation is purely dependent on the proportionality of the surface exposure of a particle; for example, a particle whose surface area is 85% chalcopyrite is considered as liberated for chalcopyrite. Furthermore, there are no hidden surprises beneath the surface as the entire particle surface, and interior mineralogy, is visible, classified, and measured. This results in liberated classifications that have no inherent assumptions, and locked classifications for mineralogies that are truly within the particle.

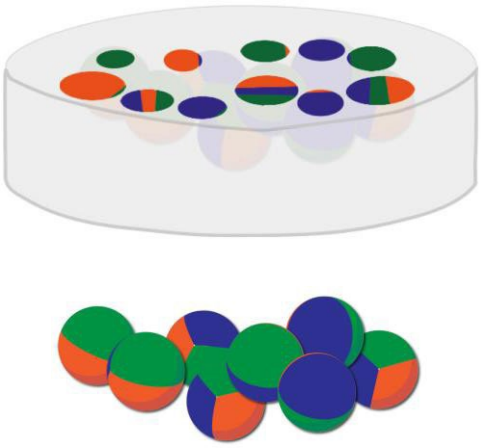

Figure 6. ***(A)*** *Mechanical alteration of the sample for SEM analysis reveals fractions of particles that the user must accept as true representations of the particle.* ***(B)*** *With X-ray microscopy, the particle's mineralogy and its exposure, or lack of, on the surface of the particle is fully recognised and measured.*

ID	Mineral	Liberated %	Middling %	Locked %	<10 %	<20 %	<30 %	<40 %	<50 %	<60 %	<70 %	<80 %	<90 %	<100 %	100 %
2	Quartz	41.03	54.21	4.76	3.23	1.53	2.0	3.46	6.24	10.07	13.5	18.94	18.96	22.03	0.04
3	Microcline	14.44	67.64	17.92	10.87	7.05	7.74	11.26	12.97	13.59	13.3	8.78	7.91	6.52	0.01
4	Calcite	45.59	32.74	21.67	15.74	5.93	4.28	7.15	7.07	3.59	4.74	5.92	10.54	34.96	0.1
5	Epidote	44.46	38.28	17.26	13.68	3.58	4.56	3.36	6.75	6.51	4.71	12.38	10.52	33.92	0.01
6	Biotiteannite	62.6	31.33	6.07	4.97	1.1	1.28	1.79	0.23	8.34	10.65	9.04	19.81	41.74	1.05
7	Pyrite	81.63	12.66	5.71	4.47	1.24	1.11	0.62	1.51	0.5	3.65	5.26	5.04	75.38	1.21
8	Chalcopyrite	7.79	56.04	36.17	21.75	14.42	6.35	14.52	0.0	16.22	9.07	9.89	7.15	0.57	0.08
9	Hematite	0.0	17.92	82.08	24.73	57.34	15.73	2.2	0.0	0.0	0.0	0.0	0.0	0.0	0.0
10	Sphalerite	0.0	0.0	100.0	100.0	0.0	0.0	0.0	0.0	0.0	0.0	0.0	0.0	0.0	0.0
11	Covellite	0.0	0.0	100.0	100.0	0.0	0.0	0.0	0.0	0.0	0.0	0.0	0.0	0.0	0.0
12	Bornite	0.0	5.68	94.32	54.68	39.65	5.68	0.0	0.0	0.0	0.0	0.0	0.0	0.0	0.0
13	Chalcocite	0.0	0.0	100.0	61.55	38.45	0.0	0.0	0.0	0.0	0.0	0.0	0.0	0.0	0.0

Figure 7. *Liberation based on the mineral's exposure on the surface of the particle and weighed by volume.*

Associations

In the 3D world, associations are measured relative to the contact of surfaces between minerals, rather than the linear contact observed in SEM analyses. Of course, a locked grain in the particle affects the association measurement in a way that cannot be measured by 2D techniques.

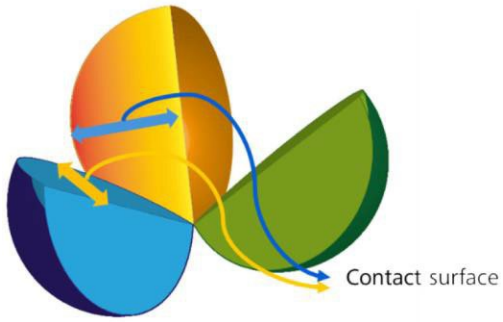

Figure 8. *Particle split open to reveal the contact surfaces between minerals. It is the proportion of the surface to the total surface of the mineral in the sample that determines the level of association between the minerals.*

Summary

Benefitting from advancements in X-ray microscopy and machine learning, Mineralogic 3D represents a step change in automated mineralogy. The unique ability to study samples in 3D, with no obscured mineralogy, without stereological artifacts, and obtaining precise data for every particle opens the door to a new understanding of the geometallurgical behaviour of ores.

This article, originally published online in November, 2021, has been very slightly edited for the Geode, and slightly "de-Zeissified" to make it slightly less of an unpaid advert and more readable as information. For the full version, including expanded images and tables, go to:

file:///C:/Users/geol024/Downloads/EN_wp_Whole-particle_Liberation_Studies.pdf

The article has been reproduced in this form with the written permission of Zeiss, courtesy of Rakesh Patel (Carl Zeiss Pty. Ltd., South Africa).

Other Gems

The Enigma Diamond

In February 2022, a news release announced the auction of an unusual, large black diamond known as the Enigma Diamond. The diamond currently weighs in at 555.55 carats, and has been cut to exhibit 55 faces, as well. It was ultimately bought for €3.16 million (not a 5 in sight, not even in $U.S.) and promptly renamed the HEX.com diamond. The recurring theme of 5 in the stone was evidently inspired by the number of digits in the human hand, with specific reference to the hamsa, an amulet depicting a stylized right hand with an eye in the palm, popular in the southern and eastern Mediterranean lands (Wikipedia).

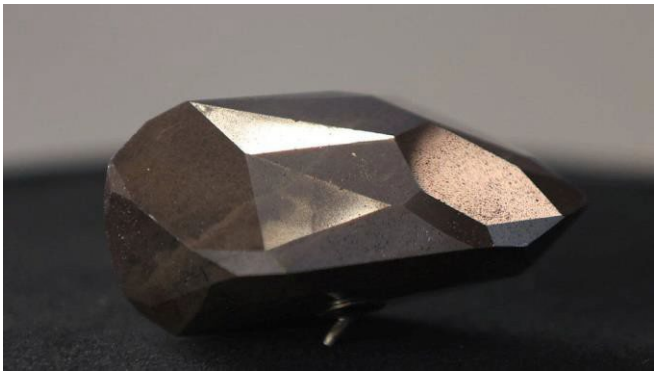

The HEX.com diamond is purported to be a prominent example of a distinctive group of black diamonds known as carbonado diamonds. Prominent amongst the hypotheses for these diamonds is a possible meteoritic origin. Accordingly, and sceptically, I solicited some thoughts from my colleagues in the meteoritical sphere for comments. My thanks to Uwe and Christian for the two articles provided here.

S. Prevec

Carbonado - The Enigma

W.U. Reimold

Institute for Geoscience, University of Brasilia, Brasilia, Brazil

On 9 February 2022 a 555.55 carat "carbonado type" black diamond, aptly dubbed The Enigma, was sold by Sothebys of London for not less than US$ 4,292,322. The company emphasized that this specimen was not only one of the largest fancy black natural-colour diamonds in the world but that it also represents the largest faceted diamond ever to have been auctioned (www.sothebys.comendigital-cataloguesthe-enigma-fancy-black-diamond). Considering that natural pieces of carbonado found in sedimentary rock exclusively in Brazil and in the Central African Republic (CAR) generally are smaller than 2 cm maximum, this much larger chunk is also one of the largest carbonado finds ever.

So, what is this carbonado? Stephen Haggerty in his 2017 review paper in Gems & Gemology summarized: "carbonado diamond represents unusual diamond aggregates that are strongly bonded but porous, contain melt-like glass patinas that cannot be found in conventional kimberlite/lamproite-derived diamonds, and are from crustal collisional settings or the possible result of meteorite impact." (ibid, vol. 53, p. 2 of the review). Carbonado may even represent the hardest natural material known, slightly harder than diamond of igneous origin. This enigmatic material was first discovered in 1841 in Brazil, on the São Francisco craton, and later in the CAR on the Congo craton. Notably, both these shields were connected in the times of the supercontinents Rondinia and earlier Columbia, more than 1 billion years ago.

Interestingly, this super-hard material was a prized polishing agent that was used for drilling during the construction of the Panama Canal. Haggerty (2014) estimated that (by that time) some 2 metric tons of carbonado had been mined. The largest piece ever retrieved weighed 3,167 ct. This author reported details about the physical and chemical characteristics of some 800 specimens and concluded that they are seemingly quite similar materials. Carbonado is opaque. It is composed of randomly oriented tiny diamond crystallites, has somewhat variable colour (black to brown or pink, and even olive green). Pores are highly significant, there are glassy patinas, and highly irregular surfaces; and the polycrystallinity of carbonado all are distinct from the features of "normal" diamond. The origin of patina is debated, also in terms of a possible origin by friction melting. Carbonados contain a wide range of trace metals, metal alloys, and some unusual minerals such as moissanite (SiC) and osbornite (TiN), as both primary intergranular inclusions or crystal-controlled oriented intergrowths. These particular phases are only stable at very reduced conditions (deep in the Earth´s mantle or

perhaps in outer space). Carbonado is light in terms of stable isotopes with $\delta^{13}C$ of -24-31 ‰ and $\delta^{15}N$ of -3.6-12.8 ‰. These data strongly distinguish carbonado from conventional diamonds.

Brazilian carbonado derived from conglomerate host rock that indicated reworking for at least 1.7 Ga (maybe right up to Meso-/Early Archean times) has been dated – directly on the diamond phase – by HR-TIMS and SHRIMP analysis. Pb-Pb ages obtained on carbonado range from 2.6-3.8 Ga, similar to ages obtained for crust-derived inclusions and the general age range for the basement of the São Francisco craton. Haggerty summarizes: carbonado is similar to conventional quenched Type Ib diamonds and chemical vapor deposited (CVC) diamond that both contain appreciable hydrogen – but carbonado has the following major differences from conventional diamond: porosity and patina, and the strongly reduced C and N isotopic character. In addition, carbonado has never been found in typical diamond-bearing mantle-derived rock.

This enigmatic material has given rise to a number of hypotheses regarding its formation/origin:

1. Since 1985 it has been debated whether meteorite impact could be responsible for carbonado formation (see Koeberl, this issue, for a more in-depth discussion). It was initially proposed that the large MagSat anomaly on the northern Congo craton (Bangui anomaly) could be the locus for a huge impact structure. Others suggested that a large meteorite impact into organic material could have resulted in carbonado with its isotopically light character. And in recent years innovative ideas about carbon-rich extraterrestrial bodies have been bandied around as possible sources of impact-derived diamondiferous material.

2. Growth and sintering in the Earth´s crust or mantle related to C-saturated fluids, which could reduce the stability conditions for diamond at some 200 km depth or more. A major issue is, however, that such fluids would be strongly oxidizing. It has also been suggested that carbonado genesis could be related to that of “framesite”, which is found in mantle-derived kimberlite (*e.g.*, in Yakutia of Russia) but this phase does not have pores and patina, and does not have the strongly reduced accessory phases.

3. A subduction related origin is seemingly also unlikely based on the physical and textural characteristics of carbonado and such subduction related diamond. No link of carbonado to mantle minerals has ever been reported.

4. Radioactive ion implantation of carbon substrates has been proposed for carbonado genesis but is extremely unlikely considering the sizes of carbonado “bodies”.

In conclusion, and as also discussed in the companion contribution by Christian Koeberl, carbonado genesis remains, for now, an enigma.

Thanks to Stephen Haggerty, and Peter Heaney and co-authors, for their excellent reviews. Tatyana Shumilova provided some pertinent information and literature. For additional information, the reader is referred to these sources:

Heaney, P.J., Vicenzi, E.P., and De, S., 2005, Strange diaonds: The mysterious origins of carbonado and framesite. ELEMENTS 1, 85-99.

Haggerty, S.E., 2014. Carbonado: Physical and chemical properties, a critical evaluation of proposed origins, and a revised genetic model. Earth-Science Reviews, 130, 49-72.

Haggerty, S.E., 2017, Carbonado diamond: A review of properties and origin. Gems & Gemology, 53, No. 2. www.gia.edu/gems-gemology/summer-2017-carbonate-diamond

Sano, Y., Yokochi, R., Terada, K., Chaves, M.L., Minoru Ozima, 2002. Ion microprobe Pb-Pb dating of carbonado, polycrystalline diamond. Precambrian Research 113, 155-168.

Shumilova, T.G., Tchakev, S.N., Shevchuk, S.S., Rappenglück, M.A., Kazakov, V.A., 2016. A “diamond-like” star in the lab. Diamond-like glass. Carbon 100, 703-709.

Carbonado: Unusual Diamonds of Disputed Origin

Christian Koeberl

Department of Lithospheric Research, University of Vienna, Austria

Recent media reports related to the auction of a large black diamond called "Enigma", which was listed by the auction house as a so-called "carbonado" diamond, and supposedly of extraterrestrial origin, caused some attention all over the world - not only related to the eventual sales price. It also has to be noted that – at least not publicly – no mention was made of any scientific studies or analyses that would support the claim that this object was really a diamond, and one of the carbonado subtype; in addition, it was simply claimed, without any evidence, that carbonados are of extraterrestrial origin. While this has been proposed at one point, it by no means the only hypothesis for the origin of carbonados, nor the most likely one.

So before coming back to the characteristics and possible origin of carbonados, it might be pertinent to discuss the properties of diamonds actually known to be of either extraterrestrial (meteoritic) origin or related to meteorite impact events. There are two sub-groups, on the one hand, diamonds that formed from other varieties of carbon by shock (which can occur both in meteorites or in meteorite craters), and very small diamonds, mostly in the nanometer regime, that probably formed in vapor processes, which can also occur in meteorites or some impact deposits.

Shock-produced diamonds (sub-mm to mm-sized, which clearly have been produced from graphite in the target rocks) have been identified at a large number of established impact structures, where they provide definite evidence of impact (Hough et al., 1995; Gilmour, 1998; Masaitis, 1998; Gilmour et al., 2003). For example, there was a detailed study by Koeberl et al.(1997) about large polycrystalline diamonds in impactites from the Popigai impact structure (Russia), which have mineralogical and crystallographic characteristics that are very similar to those of graphites found in the graphite-bearing precursor gneisses. This indicates that these diamonds most likely formed by shock-induced solid-state (martensitic) transformation of graphite to diamond. As described by Koeberl et al. (1997), this transformation seems to have occurred between about 35 and 60 GPa (on the basis of petrographic observations of shock phenomena in the host rocks). The size of the individual crystallites making up the polycrystalline diamond is mostly less than one micrometer, and transmission electron microscopic studies show the presence of abundant thin lamellae. In addition, some of these diamonds contain minor inclusions with CO2 at high pressure, which must have been included during the high-pressure shock transformation of graphite to diamond. This observation provides additional evidence against diamond formation by chemical vapor deposition processes. Trace element and carbon and nitrogen isotopic data, as well as the low N abundances, support the conclusion that the diamonds formed in situ by shock metamorphism (Koeberl et al., 1997).

Other shock-produced diamonds are known from a variety of meteorites, mainly the carbon-rich ureilite meteorites (e.g., Lipschutz, 1964; Nestola et al., 2020), for which earlier also static high pressure formation models were discussed, but the more recent work showed them to be of shock meteomorphic origin as well. Some meteorites contain so-called nanodiamonds, which are also found at some impact sites; their origin is less clear. These diamonds, which occur as crystals typically 3–5 nm in size, occur in some meteorites and can also be synthesized at low pressures by a variety of nonequilibrium chemical-vapor-deposition (CVD) techniques (e.g., Gilmour, 1998), and their formation and relation to terrestrial impact events is still not clear. What is clear is that they cannot be used as evidence for an impact origin of any disputed structure or deposit, but they do occur in finely dispersed form in some meteorites.

In contrast, carbonado is an enigmatic polycrystalline diamond variety found in placer deposits in Brazil and the Central African Republic (e.g., Trueb and Butterman, 1969; Heaney et al., 2005, Ketcham and Koeberl, 2013, and references therein). Carbonados are mostly millimeter to centimeter sized, and age determinations range from 2.6 to 3.8 Ga, with large uncertainties (e.g., Sano et al., 2002). The limited geographic distribution of carbonados, on land masses that were likely adjacent at times in the Archean, suggests that they may all have been created in a single event (Heaney et al., 2005). Carbonados have, compared to other diamond varieties, some unusual characteristics. They are texturally diverse, often very porous, and consisting of small (10–250 µm) diamonds cemented together by even smaller (<1 µm) microdiamonds that may have subplanar dislocations that may be interpreted as defect lamellae, whereas

the larger ones are mostly defect free. In terms of carbon isotopic composition, carbonados are very light, with δ13C values ranging from –21‰ to –32‰, which is rare for diamonds and suggestive of organic carbon (see references in Ketchan and Koeberl, 2013). Some carbonado material has been found to be enriched in isotopes characteristic of the products of spontaneous fission of uranium (e.g., Sano et al., 2002), but cathodoluminescence imaging suggests that this may be a secondary feature caused by infiltration of the pore network by fluids enriched in radioactive elements (see references in Heaney et al., 2005, and Ketcham and Koeberl, 2013).

The inclusion suite in carbonado is also somewhat enigmatic. Carbonados have been found to contain nanoinclusions of various metal alloys (Fe, Fe-Ni, Ni-Pt, Si, Ti, Sn, Ag, Cu, and SiC), as well as some minerals (calcite, sylvite, smithsonite) that may be original or even some (augite, ilmenite, phlogopite) that may predate the diamond-forming event (see references in Ketcham and Koeberl, 2013); there are also larger metal particles that are tens of micrometers in diameter within open pore space. In terms of macro-inclusions, there are minerals of possible crustal origin, such as orthoclase, goethite, quartz, kaolinite, hematite, serpentine, and florencite, a hydrous rare-earth phosphate that commonly forms as an alteration product of monazite. Computer tomography work by Ketcham and Koeberl (2013) indicated, in agreement with other recent observations, that carbonados most likely crystallized from a carbon-supersaturated fluid and suggest that the second stage may correspond with the creation of the pore alignment fabric, with most present-day macroinclusions being mostly secondary. Any earlier suggestions that carbonados formed either by impact or are of extraterrestrial origin (*e.g.*, Garai *et al.*, 2005) have not been supported by more recent investigations, and thus the source of the "Enigma" diamond remains an enigma….

References

Garai, J., Haggerty, S.H., Rekhi, S., and Chance, M., 2006, Infrared absorption investigations confirm the extraterrestrial origin of carbonado diamonds: The Astrophysical Journal, v. 653, no. 2, p. L153–L156, doi:10.1086/510451.

Gilmour, I., 1998. Geochemistry of carbon in terrestrial impact processes. In: Grady, M.M., Hutchison, R., McCall, G.J.H. (Eds.), Meteorites: Flux with Time and Impact Effects. Geological Society Special Publication, vol. 140. Geological Society, London, pp. 205–216.

Heaney, P.J., Vicenzi, E.P., and De, S., 2005, Strange diamonds: The mysterious origins of carbonado and framesite: Elements, v. 1, p. 85–89, doi:10.2113/ gselements.1.2.85.

Hough, R.M., Gilmour, I., Pillinger, C.T., Arden, J.W., Gilkes, K.W.R., Yuan, J., Milledge, H. L., 1995. Diamond and silicon carbide in impact melt rock from the Ries impact crater. Nature 378, 41–44.

Ketcham R.A. and Koeberl C. (2013) New textural evidence on the origin of carbonado diamond: An example of 3-D petrography using X-ray computed tomography. Geosphere 9, 1336-1347.

Koeberl, C., Masaitis, V.L., Shafranovsky, G.I., Gilmour, I., Langenhorst, F., and Schrauder, M. (1997) Diamonds from the Popigai impact structure, Russia. Geology 25, 967-970.

Lipschutz M.E. (1964) Origin of diamonds in the ureilites. Science 143, 1431–1434.

Masaitis, V.L., 1998. Popigai crater: origin and distribution of diamond-bearing impactites. Meteoritics and Planetary Science 33, 349–359.

Nestola, F., Goodrich, C.A., Morana, M., Barbaro, A., Jakubek, R.S., Christ, O., Brenker, F.E., Domeneghetti, M.C., Dalconi, M.C., Alvaro, M., Fioretti, A.M., Litasov, K.D., Fries, M.D., Leoni, M., Casati, N.P.M., Jenniskens, P., & Shaddad, M.H. 2020. Impact shock origin of diamonds in ureilite meteorites. Proc. Natl. Acad. Sci. U.S.A.; 117(41): 25310-25318. doi: 10.1073/ pnas. 1919067117.

Sano, Y., Yokochi, R., Kentaro, T., Chaves, M.L., and Ozima, M., 2002, Ion microprobe Pb-Pb dating of carbonado, polycrystalline diamond: Precambrian Research, v. 113, p. 155–168, doi:10.1016/S0301-9268(01)00208-X.

Trueb, L.F., and Butterman, W.C., 1969, Carbonado: A microstructural study: The American Mineralogist, v. 54, p. 412–425.

Minsa invites its members to contribute submissions for our next issue of the Geode, on the theme of "*Analytical data sources for you and your students*" (see below), for June 2022.

Submissions can be sent to minsa@gssa.org.za and should reach us by 31st May 2022.

Where are you getting your analytical data from these days, whether it is for Honours projects (even "teaching-research" needs real data), M.Sc. and Ph.D. studies or your own non-student-driven research projects (is there such a thing?), or for consulting work. What are your sources of suitably high quality, sufficiently rapidly turned-around, cost effective analytical data for the geosciences. Tell us why you are using them (we don't need to hear, at least not in print, why you are not using specific alternative potential sources; give us the good news only).

Earn CPD points through mentoring!

BridgeTheGap
GeosciencesGuidanceProgram
EMPOWER || INSPIRE

MINSA

Be "the mentor you wish you had" and assist in giving some guidance to geology students by signing up to be a mentor through the Bridge the Gap Geosciences Guidance Program (BTG).

BTG is a student run organisation that focuses primarily on mentorship between undergraduate and postgraduate students. However, all interested individuals are invited to "bridge the gap" between students and industry by joining the BTG program. This could take the form of mentorship, giving a talk, leading an excursion or simply providing sponsorship.

To get involved please complete the Google form via this link: https://forms.gle/Sf5tMciuSStAQuFL8 or email bridgethegap.wits@gmail.com for more information.

Applied heat loss in everyday life

or

Based on the thermometer readings at the entrance to my local grocery store, how long have I been dead?

"Normal" body temperature is 34.2° to 37.6° with a mean of around 36.9°C. This may vary by individual according to various circumstances. Elevated temperatures can be a byproduct of exertion, infection, stimulants, and dehydration, among other things. Decreased temperatures can be caused by hyperthyroidism, frailty syndrome, or hypothermia. Or death. These could all be reasonably described as in some way "abnormal" conditions, then.

Stage 1 hypothermia, where the body temperature is between 32-35°C (typical grocery store measurement range), is characterised by disorientation and confusion, shivering, and increased frequency of need to urinate. These symptoms also go with excessive beer consumption (if you're sitting under the air conditioning). With both advanced hypothermia, and with beer consumption, unaccountably removing one's clothes is a symptom that things have gone too far.

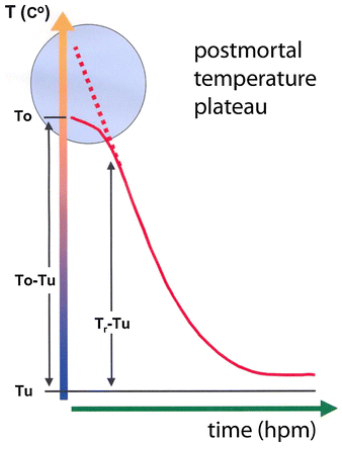

The body maintains its life temperature for between 1-3 hours after death as chemical reactions continue, although with decreasing amounts of oxygen available, subsequently declining according to a rate dictated by the ambient temperature (so in effect the temperature gradient between the body and its surroundings), your degree of insulation (how well-clad you are), and other factors such as whether there is a breeze or not. In general, by 18-20 hours your body has achieved a thermal equilibrium with your surroundings, losing heat by about 1°C per hour on average (although based on the factors, could be between 0.5 and 1.5°C/hr).

Rigor mortis, which is the stiffening of joints and muscle fibres, triggered by the unavailability of oxygen for the energy-producing reactions in the muscle fibre cells, sets in after 3-4 hours, and only wears off after about 2 days as the cell fibres begin to break down.

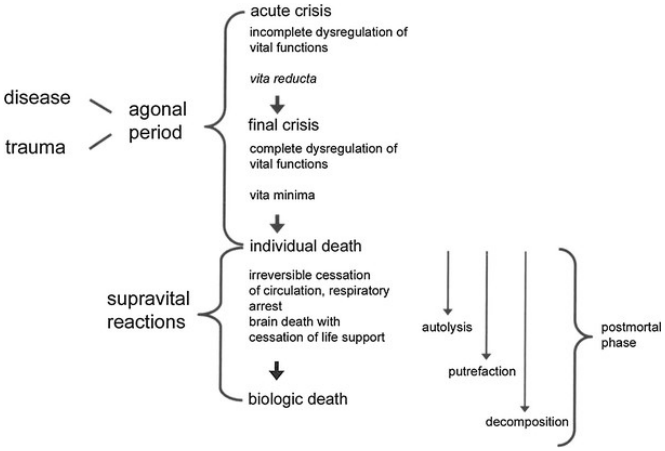

Putrefaction is the breakdown of the body's proteins through reaction with water, forming amino acids (hydrolysed proteins) and gases. Body odour on a living person comes from bacterial interactions with enzymes (fatty acids, generally, which are not quite the same thing as proteins) secreted from glands under our skin. To quote Wikipedia here, this causes "male armpits to give off of a rancid/cheese-like smell whereas female armpits give off a more fruity/onion-like smell". Puppy dog tails vs. sugar and spice, etc.

So, if I go to the shops on a summer afternoon, with an ambient air temperature of 28°C, and a measured body temperature (non-rectally; even at Woolworths, they don't let you use the changing rooms for that) of 34.5°C, at my current weight (the bulkier you are, the longer it takes you to shed body heat, as you might expect), I'd have been dead for 11 hours, plus or minus 2.8 hours. This would be likely consistent with the body odour after working from home for a week during Stage 3 lockdown, and the stiffness in my limbs from absence of exercise punctuated by lifting 20 litre jugs of potable water up to the counter top, in lieu

of a reliable municipal water supply, rendering me incapable of bending down to pick up any item worth less than R20 on short notice. I can be thus be reasonably assessed to be somewhere in mid-postmortem, semi-putrefied. Until I get to the next store, and get a 36.5°C. Or a 33.2°C. If you plot your daily measurements and get a linear downwards curve of temperature vs. time, you might want to have a little lie down.

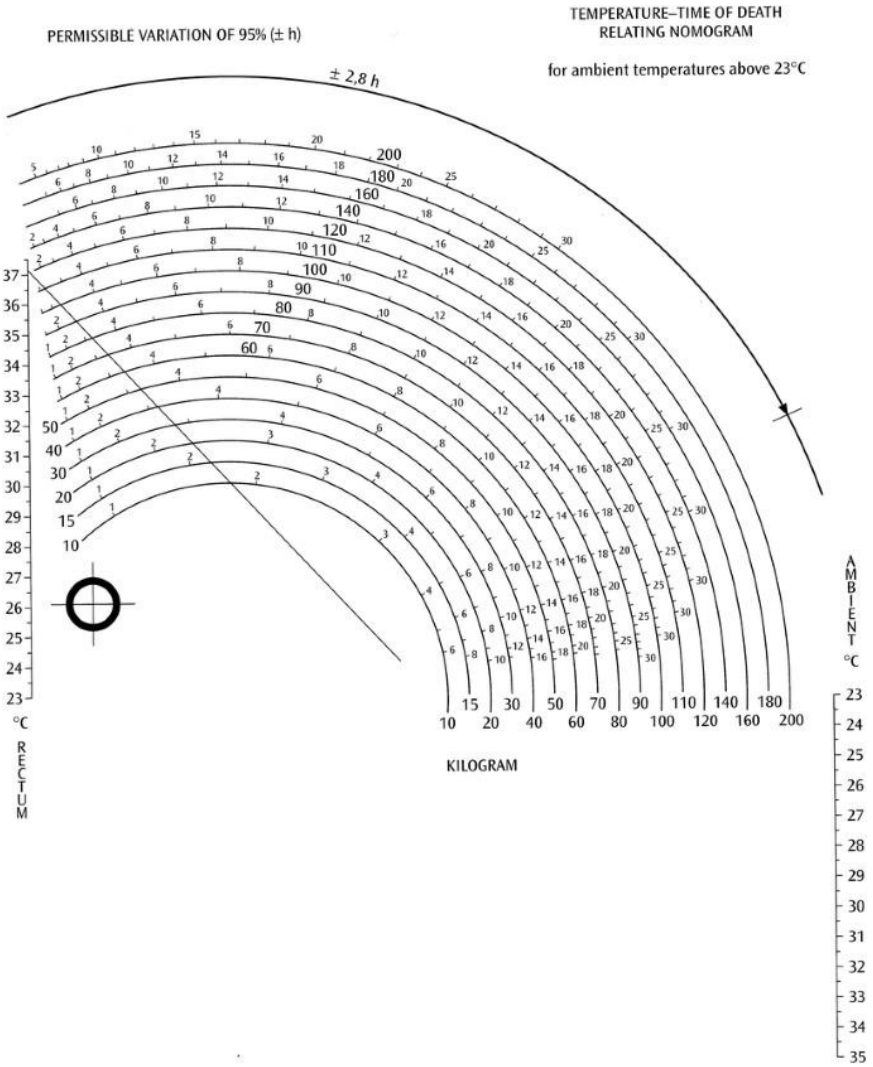

The Hensgge nomogram is used to provide a some-what nuanced estimation of time since death, at which point your hypo-thalamus (it's in your brain) stops regulating your body temperature for you.

The body temperature is based on rectal temperature, and specifically "deep rectal temperature" (defined as at least 8 cm), if you were thinking that the current optimal COVID testing method is overly invasive. There can be up to a 1-2 degree difference between core and external temperature measurements.

Sources:

Madea, B. (2016) Methods for determining time of death. Forensic Science, Medicine, and Pathology 12, 451–485.

Various authors in (2018) Algor Mortis: Forensic Ecogenomics. https://www.sciencedirect.com/topics/medicine-and-dentistry/algor-mortis#

Contributed by S. Prevec

IMA 2022

MINERALOGY AND SPACE

Lyon, 18-22 July

Following the tradition of quadri-annual general meetings of the International Mineralogical Association organized by national societies, the French Society for Mineralogy and Crystallography will host the 23rd general meeting of the IMA in Lyon, France during 18-22 July 2022.

2022 is the year to celebrate mineralogy. It marks the bicentennial of the death of René Just Haüy (born 1743) who is a father of modern mineralogy and crystallography. Two centuries ago is also when Haüy's Traité de mineralogy and Traité de cristallographie were published. Back to our days, in 2022, the last two main Mars exploration programs, Perseverance (Mars2020) and Huoxing 1, will just have had enough time for science return and post-processing. With the return of Hayabusa 2, for the first time, fragments of a primitive carbonaceous asteroid will be analysed.

The 23rd meeting of the IMA will mark these celebrations. In Lyon, we want to paint IMA 2022 with the colours of space exploration. Alongside the more traditional mineralogist we want to inspire the new generation and make a step closer toward the final frontier. The meeting will bring together all the new facets of modern mineralogy; it will be the playground where mineralogy as we know it will meet exploratory planetology, and it will be the place to celebrate two centuries of mineralogy.

The overarching themes of the IMA2022 are:

* Mineral Systematics
* Physics and Chemistry of Minerals
* Ores and Ore Mineralogy
* Mineralogy and Petrology
* Planetary Mineralogy
* Planetary Interiors
* The Dynamical World Of Minerals

To stay updated visit regularly the official conference website: https://ima2022.fr and follow us on Facebook and twitter. The venue is the Lyon Convention Centre, a state-of-the-art, impressive convention centre featuring 25,000m² of innovative architecture and situated between the Rhône river and the Tête d'Or Park.

On behalf of the French Society for Mineralogy and Crystallography, the leading committee is formed of Razvan Caracas, Herve Cardon, and Cathy Quantin-Nataf.

We are looking forward to seeing you in Lyon in 2022!

Bruce's Beauties: Smithsonite

Smithsonite, $ZnCO_3$, was named in 1832 by François Sulpice Beudant in honour of James Smithson (1754-1829), British chemist, mineralogist, and benefactor of the Smithsonian Institution in Washington, DC, USA (Mindat.org). Smithsonite occurs most commonly as colourless rhombohedral crystals. However, traces of other elements such as copper, cobalt and cadmium can impart colourful varieties. The specimens featured here are from two well-known Namibian mines that have produced a wide variety of aesthetic crystals.

A cavity in sulphide ore lined by pink cobalt-rich smithsonite, 13.5 cm. Tsumeb mine Namibia. Bruce Cairncross specimen and photo ©.

Pale green copper-rich smithsonite, on white dolomite, with a single, twinned cerussite, 4.2 cm. Tsumeb mine, Namibia. Bruce Cairncross specimen and photo ©.

A 12 cm cabinet-sized specimen of cadmium-rich rhombohedral smithsonite. Tsumeb mine, Namibia. Bruce Cairncross specimen and photo ©.

Figure 4. Pale blue dumbbell-shaped smithsonite from the Skorpion mine in southern Namibia. Bruce Cairncross specimen and photo ©.

Minsa Crossword for March 2022

This issue's crossword theme is polymorphs. Some are common, some obscure. Test your knowledge of the little brothers and sisters of the more well-known minerals. Only those with actual names will qualify here; α, β, δ forms of minerals that nobody could even be bothered to name after somebody will not be entertained. Personally I thought I would find a lot more of these out there; if anyone can suggest some more minerals that feature them, your name will go into a hat, and the winner gets a (used, but a nice one) t-shirt (I have a lot of them). E-mail s.prevec@ru.ac.za with subject "polymorphs"!

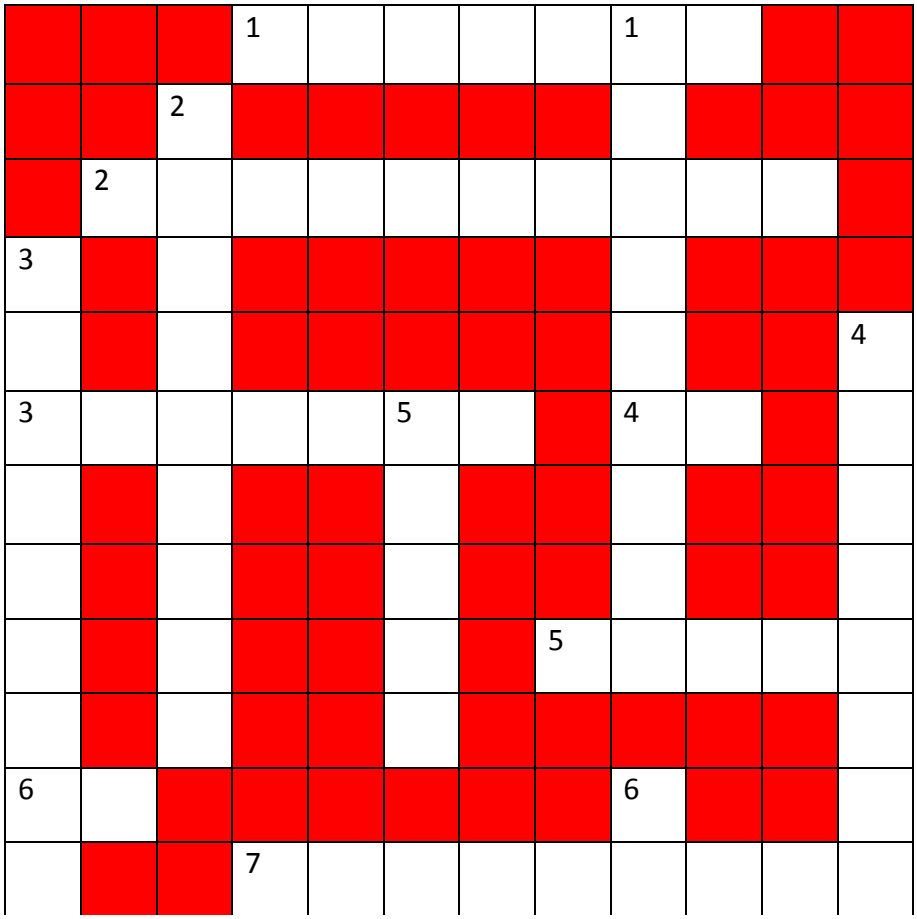

ACROSS:

1. A high-pressure (>30 GPa) polymorph of zircon associated with impact craters, named in 2002.
2. A high-pressure form of Mg_2SiO_4 first found in a meteorite. Not as high pressure as Ringwoodite, but similarly able to incorporate H into the structure and potentially hold water.
3. A low-temperature metastable polymorph of brookite and akagoiite.
4. The cation typically present in 3 DOWN whose presence stabilizes this polymorph at low temperatures and pressures.
5. The total number of SiO_2 polymorphs; don't forget the 'new' one in 4 DOWN.
6. The primary cation in the minerals in 3 ACROSS.
7. The informal name for the spherical structural polymorphs of graphite and diamond formed at high temperatures but low pressures, found associated with wildfires.

DOWN:

1. A high temperature polymorph of quartz normally associated with felsic volcanism; the Curiosity Rover unexpectedly found some on Mars in 2015.
2. The polymorph of FeS_2 that forms under particularly acidic conditions. Jewellery made of its polymorph is, confusingly, referred to by this mineral name.
3. The high pressure form of $CaCO_3$ that also, paradoxically, is the preferred polymorph for biomineralization, probably because of the ion in 4 ACROSS.
4. A polymorph of SiO_2 rejected by the IMA in 1994 as being too similar to quartz, accepted 5 years later (it's biaxial!); found in rhyolitic ignimbrite in the Canary Islands.
5. The category of metamorphism in which the mineral found in 1 ACROSS can form.
6. Prograde metamorphism of muscovite and quartz (in the absence of water) produces a polymorph of Al_2SiO_5, melt, and this mineral, whose abbreviation we seek. Yes, I know it's a stretch. As a consequence of this reaction in the Bushveld contact aureole, South Africa has the world's largest ore reserves of andalusite.

Minsa Crossword Solution for December 2021

Last issue's crossword theme was "minerals beginning with "A". We here in the Editorial office are aware that this was lame.

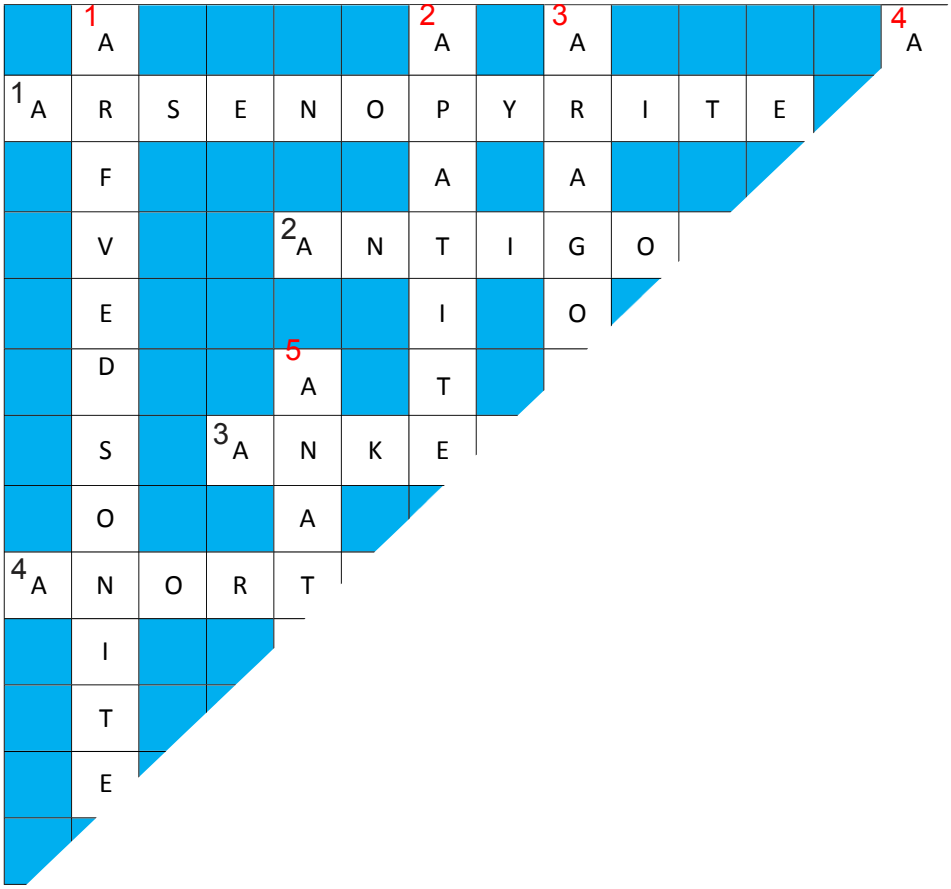

ACROSS:

1. A major ore of arsenic, it is also commonly associated with gold.
2. A variety of serpentine.
3. An Fe and Mn-rich dolomite-like carbonate mineral.
4. The most calcic species of plagioclase feldspar.
5. A sodic clinopyroxene, also formerly known as acmite.

DOWN:

1. Sodic amphibole found in nepheline syenites.
2. The main phosphate mineral in rocks.
3. A structural polymorph of Mg-bearing calcite.
4. The plagioclase feldspar found in massif-type anorthosites (extending the "A" theme).
5. A polymorph of rutile.
6. Technically not a mineral, but an amorphous organic resin.

Note: The recommended deadline for submissions for the next issue of the Geode is May 31, 2022.